STATISTICAL ANALYSIS OF JOINTLY-OPTIMIZED GSC IMPLEMENTATIONS OF BEAMFORMER-ASSISTED ACOUSTIC ECHO CANCELERS

*M. H. Maruo *, J. C. M. Bermudez †, L. S. Resende*

Department of Electrical Engineering
Federal University of Santa Catarina, 88040-900, Florianópolis, SC, Brasil
Emails: {maruo, j.bermudez, resende}@ieee.org

ABSTRACT

Beamformer-assisted acoustic echo cancelers have raised a lot of interest lately. The same performance can be obtained with a reduced length acoustic echo canceler (AEC) as the beamformer (BF) performs spatial cancellation. Structures that jointly optimize the BF and the AEC coefficients are preferred in order to exploit synergies. Analytical models have been already derived for the behavior of the direct form implementation of such systems adapted using the constrained least-mean square (CLMS) algorithm. This work extends the analysis to the popular generalized sidelobe canceler (GSC) structure, while allowing for a positive definite step-size matrix. Analytical models are derived for the mean and mean-square behaviors of the adaptive coefficients. Simulation results are shown to be in excellent agreement with the performance predicted by the theory.

Index Terms— Acoustic echo cancellation, microphone arrays, adaptive filtering, beamforming, statistical analysis

1. INTRODUCTION

Acoustic echoes arise when a microphone picks up the signal radiated by a loudspeaker and its reflections at the borders of a reverberant environment. Without a handset to provide attenuation between loudspeaker and microphone, intelligibility and listening comfort degrade [1, 2]. Typical room reverberation times require adaptive acoustic echo cancelers with very long responses [1, 2]. Fast convergence and satisfactory echo cancellation are hard to obtain under these conditions [1–4].

The desired speech signal is usually corrupted by speech from other talkers, noise and echoes in an acoustic environment. Spatial filtering (beamforming) can help attenuate interfering signals in directions other than the direction of arrival (DOA) of the desired speaker. Beamformers (BF) have limited echo suppression capacity due to limits in the array directivity [5] and the large number of microphones necessary to suppress all reflections outside the desired DOA [6].

Acoustic echo cancellation solutions in which BFs and acoustic echo cancelers (AECs) have complementary functions have raised a lot of interest recently [7–15]. BFs and AECs contribute by different means to reduce the residual echo. Hence, using both techniques in a synergistic way can improve the acoustic echo cancellation performance. BFs an AECs are usually combined by means of two basic structures [7]. The AEC first structure (AEC-BF) employs one AEC per microphone [15]. The BF then processes the AEC outputs for spatial filtering. It requires several long AECs, leading to very high computational costs [15]. Moreover, signals not in the desired DOA must be treated as double talk, complicating the design. The BF first (BF-AEC) structure does the spatial filtering first, leaving basically the echo in the desired DOA to be canceled by a single AEC [13, 14].

Despite the possibilities of combined BF and AEC acoustic echo cancellation systems, we find only few analyses of their transient behavior in the literature. The AEC-BF structure has been studied for the acoustic echo cancellation problem in [15] and for the acoustic feedback cancellation in [16]. A stochastic model has been derived using the power transfer function method for the case of a fixed BF, where just the AEC is adapted. More recently [13, 14], the performance of a system where BF and AEC are jointly adapted using equal and fixed step-sizes was analyzed. The analysis in [13,14] considered a beamformer implemented in the direct form. The derived analytical model was shown to accurately predict the adaptive system behavior and corroborated previous experimental findings that the same cancellation performance of a single-microphone AEC can be achieved with a shorter AEC when the possibility of spatial filtering is available [14, 17]. The model, based on the equivalence to a conventional LCMV optimization, allows the use of previous analytical results [18, 19]. Another very popular beamformer implementation employs the generalized sidelobe canceler (GSC) structure [8, 10, 12], which in certain situations leads to implementations with lower computational complexity than the direct form.

This work extends the analysis in [13,14] to the study of the transient behavior of the jointly optimized BF-AEC structure in the GSC form. We formulate the joint optimization as a single constrained optimization problem, what simplifies the statistical analysis. Moreover, the analysis is extended to the case of a positive-definite step-size matrix [20–22]. The incorporation of this extra flexibility to the model is particularly interesting for BF-assisted echo cancelers, as their AEC adaptation control logic stops AEC adaptation during double-talk periods, while the BF continues adapting. In [22] it is shown that, in the absence of noise perturbations, a LMS algorithm with matrix step-size is equivalent to a single step LMS on a transformed space. The same idea is used in our convergence analysis.

In this paper, plain lowercase or uppercase letters denote scalars, lowercase boldface letters denote column vectors and uppercase boldface letters denote matrices.

2. PROBLEM STATEMENT

Fig. 1 shows the BF-AEC structure, with M echo impulse response vectors $\mathbf{h}_m$ of length N_h, M microphone signals $x_m[n]$, one adaptive wideband beamformer composed of M filters $\mathbf{b}_m[n]$ of length

*This work was supported by CNPq under grant No 140640/2009-6.
†This work was partly supported by CNPq under grants Nos 305377/2009-4 and 473123/2009-6

978-1-4799-2893-4/14/$31.00 ©2014 IEEE

N_{BF} and an adaptive AEC filter $\hat{\mathbf{h}}[n]$ of length N_{AEC}. We assume responses $\mathbf{h}_m$ constant for mathematical tractability.

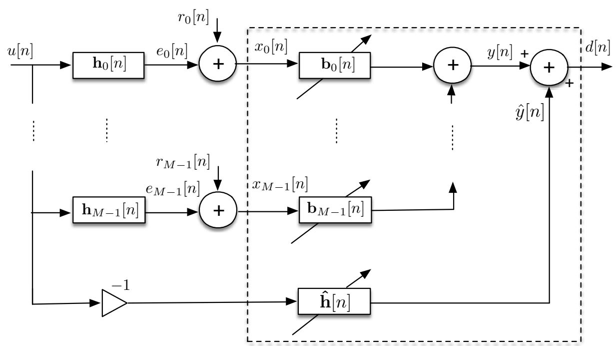

Fig. 1. BF-AEC system in the direct form structure [13].

2.1. Signal Model

The mth microphone signal $x_m[n]$ is the sum of a near-end signal $r_m[n]$ and an echo $e_m[n]$: $x_m[n] = e_m[n] + r_m[n]$. Each signal $r_m[n]$ is composed of local speech, local interferences and random noise. The echo $e_m[n]$ results from the filtering of $u[n]$ by $\mathbf{h}_m$. We define the microphone array snapshot $\boldsymbol{x}_{\mathrm{s}}[n]$ at time n as $\boldsymbol{x}_{\mathrm{s}}[n] = [x_0[n] \quad x_1[n] \quad \cdots \quad x_{M-1}[n]]^T$ and the combined beamformer input regressor as [18]

$$\boldsymbol{x}_{\mathrm{b}}[n] = \Big[\boldsymbol{x}_{\mathrm{s}}^T[n]\, \boldsymbol{x}_{\mathrm{s}}^T[n-1] \cdots \boldsymbol{x}_{\mathrm{s}}^T[n-(N_{\mathrm{BF}}-1)]\Big]^T. \quad (1)$$

Defining the vector $\boldsymbol{b}_{\mathrm{s}_\ell}[n]$ of the ℓth components of all vectors $\boldsymbol{b}_m[n]$, $m = 0, \ldots, M-1$, at time n as

$$\boldsymbol{b}_{\mathrm{s}_\ell}[n] = \Big[b_{0_\ell}[n]\, b_{1_\ell}[n] \cdots b_{M-1_\ell}[n]\Big]^T,\ \ell = 0, \ldots, N_{\mathrm{BF}}-1$$

we write the beamformer output $y[n] = \sum_{\ell=0}^{N_{\mathrm{BF}}-1} \boldsymbol{x}_{\mathrm{s}}^T[n-\ell]\boldsymbol{b}_{\mathrm{s}_\ell}[n]$. Now, defining the stacked beamformer weight vector

$$\boldsymbol{b}[n] = \Big[\boldsymbol{b}_{\mathrm{s}_0}^T[n] \quad \boldsymbol{b}_{\mathrm{s}_1}^T[n] \quad \cdots \quad \boldsymbol{b}_{\mathrm{s}_{N_{\mathrm{BF}}-1}}^T[n]\Big]^T \quad (2)$$

and using (1), we write $y[n]$ as the linear filtering $y[n] = \boldsymbol{b}^T[n]\boldsymbol{x}_{\mathrm{b}}[n]$.

Next, defining the AEC response vector

$$\hat{\boldsymbol{h}}[n] = \Big[\hat{h}_0[n] \quad \hat{h}_1[n] \quad \cdots \quad \hat{h}_{N_{\mathrm{AEC}}-1}[n]\Big]^T \quad (3)$$

and the AEC input vector $\boldsymbol{u}_{\hat{\mathrm{h}}}[n] = [u[n] \cdots u[n-(N_{\mathrm{AEC}}-1)]]^T$ yields $\hat{y}[n] = \hat{\boldsymbol{h}}^T[n]\boldsymbol{u}_{\hat{\mathrm{h}}}[n]$. The residual echo is $d[n] = y[n] - \hat{y}[n]$. Finally, defining the combined input and adaptive coefficient vectors $\boldsymbol{s}[n] = [-\boldsymbol{u}_{\hat{\mathrm{h}}}{}^T[n] \ \boldsymbol{x}_{\mathrm{b}}{}^T[n]]^T$ and $\boldsymbol{w}[n] = [\hat{\boldsymbol{h}}^T[n] \ \boldsymbol{b}^T[n]]^T$, respectively, we have

$$d[n] = -\boldsymbol{u}_{\hat{\mathrm{h}}}^T[n]\hat{\boldsymbol{h}}[n] + \boldsymbol{x}_{\mathrm{b}}^T[n]\boldsymbol{b}[n] = \boldsymbol{s}^T[n]\boldsymbol{w}[n]. \quad (4)$$

2.2. Performance Surface

The mean output power (MOP) performance surface J is defined as the mean value of $d^2[n]$ conditioned on $\boldsymbol{w}[n] = \boldsymbol{w}$. From (4),

$$\begin{aligned} J = E\{d^2[n]|\boldsymbol{w}[n] = \boldsymbol{w}\} &= E\left\{\boldsymbol{w}^T\boldsymbol{s}[n]\boldsymbol{s}^T[n]\boldsymbol{w}\right\} \\ &= \boldsymbol{w}^T\boldsymbol{R}_{\mathrm{ss}}\boldsymbol{w}. \end{aligned} \quad (5)$$

where $\boldsymbol{R}_{\mathrm{ss}} = E\{\boldsymbol{s}[n]\boldsymbol{s}^T[n]\}$ is the input autocorrelation matrix. A set of N_f linear constraints on the beamformer coefficients implements the spatial filtering. Usually, an $MN_{\mathrm{BF}} \times N_f$ constraint matrix $\boldsymbol{C}$ and an $N_f \times 1$ response vector $\boldsymbol{f}$ jointly define the frequency response in the desired DOA [18, 23].

To formulate the linear constraints as a function of the combined coefficient vector, we define the extended constraint matrix [10]

$$\boldsymbol{C}_{\mathrm{e}} = \Big[\boldsymbol{0}_{N_f \times N_{\mathrm{AEC}}} \qquad \boldsymbol{C}^T\Big]^T. \quad (6)$$

Finally, the joint optimization problem can be formulated as

$$\boldsymbol{w}_{\mathrm{opt}} = \arg\min_{\boldsymbol{w}} \boldsymbol{w}^T\boldsymbol{R}_{\mathrm{ss}}\boldsymbol{w} \quad (7a)$$

$$\text{subject to } \boldsymbol{C}_{\mathrm{e}}^T\boldsymbol{w} = \boldsymbol{f} \quad (7b)$$

2.3. Implementation Using the GSC Form

In the direct form structure of Fig. 1, the solution to (7) is split into two orthogonal components

$$\boldsymbol{w} = \boldsymbol{w}_{\mathrm{feas}} + \boldsymbol{w}_{\perp} \quad (8)$$

where $\boldsymbol{w}_{\mathrm{feas}}$ satisfies (7b), and $\boldsymbol{w}_{\perp}$ is in the complementary orthogonal space of $\boldsymbol{C}_{\mathrm{e}}$. For instance, in [13, 18] the solutions are set by assigning $\boldsymbol{w}_{\perp} = \boldsymbol{P}_{\mathrm{e}}\boldsymbol{w}$ and $\boldsymbol{w}_{\mathrm{feas}} = \boldsymbol{C}_{\mathrm{e}}(\boldsymbol{C}_{\mathrm{e}}^T\boldsymbol{C}_{\mathrm{e}})^{-1}\boldsymbol{f} = [\boldsymbol{0}_{1\times N_{\mathrm{AEC}}} \qquad \boldsymbol{\xi}^T]^T$ where

$$\begin{aligned} \boldsymbol{P}_{\mathrm{e}} &= (\boldsymbol{I}_{N_{\mathrm{AEC}}+MN_{\mathrm{BF}}} - \boldsymbol{C}_{\mathrm{e}}(\boldsymbol{C}_{\mathrm{e}}^T\boldsymbol{C}_{\mathrm{e}})^{-1}\boldsymbol{C}_{\mathrm{e}}^T) \\ &= \begin{bmatrix} \boldsymbol{I}_{N_{\mathrm{AEC}}} & \boldsymbol{0}_{N_{\mathrm{AEC}}\times M.N_{\mathrm{BF}}} \\ \boldsymbol{0}_{M.N_{\mathrm{BF}}\times N_{\mathrm{AEC}}} & \boldsymbol{P} \end{bmatrix} \end{aligned} \quad (9)$$

with $\boldsymbol{P} = \boldsymbol{I}_{M.N_{\mathrm{BF}}} - \boldsymbol{C}(\boldsymbol{C}^T\boldsymbol{C})^{-1}\boldsymbol{C}^T$ and $\boldsymbol{\xi} = \boldsymbol{C}(\boldsymbol{C}^T\boldsymbol{C})^{-1}\boldsymbol{f}$.

In the GSC form [24], the dashed square of Fig. 1 is replaced by the dashed square of Fig. 2. Feasible solutions to (7) are decomposed

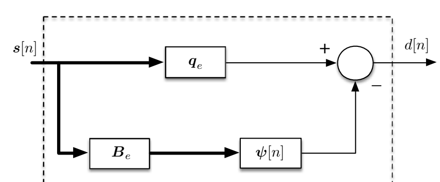

Fig. 2. BF-AEC system in the GSC configuration.

as [24]

$$\boldsymbol{w} = \boldsymbol{q}_{\mathrm{e}} - \boldsymbol{B}_{\mathrm{e}}\boldsymbol{\psi} \quad (10)$$

where $\boldsymbol{q}_{\mathrm{e}}$ is any feasible solution to (7b), $\boldsymbol{B}_{\mathrm{e}}$ is a full column-rank $(N_{\mathrm{AEC}} + MN_{\mathrm{BF}}) \times N_\psi$-dimensional blocking matrix orthogonal to $\boldsymbol{C}_{\mathrm{e}}$ ($\boldsymbol{C}_{\mathrm{e}}^T\boldsymbol{B}_{\mathrm{e}} = \boldsymbol{0}$), $\boldsymbol{\psi}$ is an N_ψ-dimensional vector and $N_\psi = N_{\mathrm{AEC}} + MN_{\mathrm{BF}} - N_f$. The minimum norm solution to (7b) is $\boldsymbol{q}_{\mathrm{e}} = \boldsymbol{C}_{\mathrm{e}}(\boldsymbol{C}_{\mathrm{e}}^T\boldsymbol{C}_{\mathrm{e}})^{-1}\boldsymbol{f}$. Both $\boldsymbol{P}_{\mathrm{e}}$ and $\boldsymbol{B}_{\mathrm{e}}$ have the same range (orthogonal to that of $\boldsymbol{C}_{\mathrm{e}}$).

2.3.1. Optimal Solution

As $\boldsymbol{C}_\text{e}^T\boldsymbol{B}_\text{e} = \boldsymbol{0}$, $\boldsymbol{w}$ in (10) satisfies (7b) for any $\boldsymbol{\psi}$, and (7) becomes an unconstrained optimization problem in $\boldsymbol{\psi}$ with solution

$$\boldsymbol{\psi}_\text{opt} = \arg\min_{\boldsymbol{\psi}} \boldsymbol{q}_\text{e}^T\boldsymbol{R}_\text{ss}\boldsymbol{q}_\text{e} - 2\boldsymbol{\psi}^T\boldsymbol{B}_\text{e}^T\boldsymbol{R}_\text{ss}\boldsymbol{q}_\text{e} + \boldsymbol{\psi}^T\boldsymbol{R}_\text{bloc}\boldsymbol{\psi} \quad (11)$$

where $\boldsymbol{R}_\text{bloc} = \boldsymbol{B}_\text{e}^T\boldsymbol{R}_\text{ss}\boldsymbol{B}_\text{e}$ denotes the blocked input autocorrelation matrix, and from (10) $\boldsymbol{w}_\text{opt} = \boldsymbol{q}_\text{e} - \boldsymbol{B}_\text{e}\boldsymbol{\psi}_\text{opt}$. Setting the gradient of (11) in respect to $\boldsymbol{\psi}$ equal to the null vector yields

$$\boldsymbol{\psi}_\text{opt} = \boldsymbol{R}_\text{bloc}^{-1}\boldsymbol{B}_\text{e}^T\boldsymbol{R}_\text{ss}\boldsymbol{q}_\text{e}. \quad (12)$$

3. STOCHASTIC GRADIENT ADAPTIVE SOLUTION

Applying a modified stochastic algorithm to search for the optimal solution (11) yields the weight update equation [24]

$$\boldsymbol{\psi}[n+1] = \boldsymbol{\psi}[n] + \boldsymbol{\mathcal{M}}\boldsymbol{B}_\text{e}^T\boldsymbol{s}[n]d[n]. \quad (13)$$

This is Eq. (30) of [24] with one important modification. We have added a positive-definite step-size matrix $\boldsymbol{\mathcal{M}}$ that can be used to control the rate of convergence and the steady-state performance of the algorithm [20–22]. The inclusion of this matrix is important because, contrary to the study in [24], the present analysis of the GSC-based structure includes the operation of both the BF and the AEC. In practical systems there exists a control logic that usually stops the AEC when double-talk occurs, while the BF continues to be adapted. Hence, BF and AEC are not always being adapted in a BF-assisted echo canceler. By including the step-size matrix $\boldsymbol{\mathcal{M}}$ in (13) we consider the possibility of using different step-sizes for the AEC and for the BF. Hence, the resulting model should be able to predict the system behavior under different possible adaptation modes.

3.1. Weight Error Vector

Define the weight error vector $\boldsymbol{v}[n] = \boldsymbol{w}[n] - \boldsymbol{w}_\text{opt}$. From (10),

$$\boldsymbol{v}[n] = \boldsymbol{q}_\text{e} - \boldsymbol{B}_\text{e}\boldsymbol{\psi}[n] - \left(\boldsymbol{q}_\text{e} - \boldsymbol{B}_\text{e}\boldsymbol{\psi}_\text{opt}\right) = -\boldsymbol{B}_\text{e}\boldsymbol{\vartheta}[n] \quad (14)$$

where $\boldsymbol{\vartheta}[n] = \boldsymbol{\psi}[n] - \boldsymbol{\psi}_\text{opt}$ denotes the weight error vector of the unconstrained filter conditioned on $\boldsymbol{B}_\text{e}$ and $\boldsymbol{q}_\text{e}$. From (14), $\boldsymbol{v}[n]$ is in the range of $\boldsymbol{B}_\text{e}$. Hence, $\boldsymbol{v}[n]$ is completely determined by $\boldsymbol{\vartheta}[n]$ conditioned on $\boldsymbol{B}_\text{e}$. We then study the behavior of $\boldsymbol{\vartheta}[n]$.

Subtracting $\boldsymbol{\psi}_\text{opt}$ from both sides of (13), using (4) with $\boldsymbol{w}[n] = \boldsymbol{v}[n] + \boldsymbol{w}_\text{opt}$ and (10) we obtain a recursive update equation for $\boldsymbol{\vartheta}[n]$:

$$\begin{aligned}\boldsymbol{\vartheta}[n+1] =& (\boldsymbol{I}_{N_\psi} - \boldsymbol{\mathcal{M}}\boldsymbol{B}_\text{e}^T\boldsymbol{s}[n]\boldsymbol{s}^T[n]\boldsymbol{B}_\text{e})\boldsymbol{\vartheta}[n] \\ &+ \boldsymbol{\mathcal{M}}\boldsymbol{B}_\text{e}^T\boldsymbol{s}[n]\boldsymbol{s}^T[n]\boldsymbol{w}_\text{opt}.\end{aligned} \quad (15)$$

4. STATISTICAL ANALYSIS

4.1. Simplifying Assumptions

We now study the behavior of BF-assisted echo canceler using (13) under the following typical simplifying assumptions:

A1 $\boldsymbol{s}[n]$ is stationary, zero-mean and Gaussian;

A2 $u[n]$ and $r[n]$ are statistically independent;

A3 $\boldsymbol{R}_\text{ss}$ is positive-definite, and both $\boldsymbol{C}_\text{e}$ and $\boldsymbol{B}_\text{e}$ have full column rank;

A4 Statistical dependence of $\boldsymbol{B}_\text{e}^T\boldsymbol{s}[n]\boldsymbol{s}^T[n]\boldsymbol{B}_\text{e}$ and $\boldsymbol{\psi}[n]$ can be neglected;

A5 The desired DOA does not change during adaptation.

Though not always valid in practice, these assumptions make analysis viable and frequently lead to results that retain sufficient information to serve as reliable design guidelines [4, p. 315],[8, 10]. Simulation results will confirm their reasonability for this analysis.

4.2. Mean Weight Error Vector Behavior

Taking the expected value of (15) under A4 and using (10) and (12) leads to $E\{\boldsymbol{B}_\text{e}^T\boldsymbol{s}[n]\boldsymbol{s}^T[n]\boldsymbol{w}_\text{opt}\} = \boldsymbol{0}_{N_\psi\times 1}$ and

$$E\{\boldsymbol{\vartheta}[n+1]\} = (\boldsymbol{I}_{N_\psi} - \boldsymbol{\mathcal{M}}\boldsymbol{R}_\text{bloc})E\{\boldsymbol{\vartheta}[n]\}. \quad (16)$$

Hence, the mean weights converge asymptotically if all eigenvalues of $\boldsymbol{\mathcal{M}}\boldsymbol{R}_\text{bloc}$ are inside the unit circle. In the following we study the second moment behavior of the weights [3].

4.3. Correlation Matrix of $\boldsymbol{\vartheta}[n]$

Post-multiplying (15) by its transpose, taking the expected value, using A1–A5, the Gaussian moment factoring theorem [4, 25], and $E\{\boldsymbol{B}_\text{e}^T\boldsymbol{s}[n]\boldsymbol{s}^T[n]\boldsymbol{w}_\text{opt}\} = \boldsymbol{0}_{N_\psi\times 1}$ yields

$$\begin{aligned}\boldsymbol{R}_{\vartheta\vartheta}[n+1] =& \boldsymbol{R}_{\vartheta\vartheta}[n] - \boldsymbol{\mathcal{M}}\boldsymbol{R}_\text{bloc}\boldsymbol{R}_{\vartheta\vartheta}[n] - \boldsymbol{R}_{\vartheta\vartheta}[n]\boldsymbol{R}_\text{bloc}\boldsymbol{\mathcal{M}} \\ &+ [J_{\min} + \text{tr}(\boldsymbol{R}_\text{bloc}\boldsymbol{R}_{\vartheta\vartheta}[n])]\boldsymbol{\mathcal{M}}\boldsymbol{R}_\text{bloc}\boldsymbol{\mathcal{M}} \\ &+ 2\boldsymbol{\mathcal{M}}\boldsymbol{R}_\text{bloc}\boldsymbol{R}_{\vartheta\vartheta}[n]\boldsymbol{R}_\text{bloc}\boldsymbol{\mathcal{M}}\end{aligned} \quad (17)$$

where $\boldsymbol{R}_{\vartheta\vartheta}[n] = E\{\boldsymbol{\vartheta}[n]\boldsymbol{\vartheta}^T[n]\}$.

4.4. Mean Output Power

The MOP is given by $J[n] = J_{\min} + \text{tr}(\boldsymbol{R}_\text{vv}[n]\boldsymbol{R}_\text{ss})$ [13] where $\boldsymbol{R}_\text{vv}[n] = E\{\boldsymbol{v}[n]\boldsymbol{v}^T[n]\}$. As $\boldsymbol{R}_\text{vv}[n] = \boldsymbol{B}_\text{e}\boldsymbol{R}_{\vartheta\vartheta}[n]\boldsymbol{B}_\text{e}^T$ from (14),

$$J[n] = J_{\min} + \text{tr}(\boldsymbol{R}_{\vartheta\vartheta}[n]\boldsymbol{R}_\text{bloc}) \quad (18)$$

5. CONVERGENCE ANALYSIS

Classical convergence analysis of (17) would project $\boldsymbol{R}_{\vartheta\vartheta}[n]$ into the eigenspace of $\boldsymbol{R}_\text{bloc}$ and study the convergence of the diagonal entries of the transformed matrix [3]. The presence of $\boldsymbol{\mathcal{M}}$ however requires a different approach, as (17) is not diagonalizable by the same projection since $\boldsymbol{\mathcal{M}}\boldsymbol{R}_\text{bloc} \neq \boldsymbol{R}_\text{bloc}\boldsymbol{\mathcal{M}}$ [26, p. 558]. Nevertheless, it is still possible to diagonalize both $\boldsymbol{\mathcal{M}}$ and $\boldsymbol{R}_\text{bloc}$ through contragradient diagonalization [26, p. 465],[27, p. 466]. As $\boldsymbol{\mathcal{M}}$ is positive definite, Cholesky decomposition yields $\boldsymbol{\mathcal{M}} = \boldsymbol{L}\boldsymbol{L}^T$ with $\boldsymbol{L}$ non-singular. Then, we can transform the vector space into $\boldsymbol{\xi}[n] = \boldsymbol{L}^{-1}\boldsymbol{\vartheta}[n]$, $\boldsymbol{R}_\text{mod} = \boldsymbol{L}^T\boldsymbol{R}_\text{bloc}\boldsymbol{L}$, and $\boldsymbol{R}_{\xi\xi}[n] = \boldsymbol{L}^{-1}\boldsymbol{R}_{\vartheta\vartheta}[n]\boldsymbol{L}^{-T}$. Pre-multiplying (17) by $\boldsymbol{L}^{-1}$ and post-multiplying by $\boldsymbol{L}^{-T}$ yields

$$\begin{aligned}\boldsymbol{R}_{\xi\xi}[n+1] =& \boldsymbol{R}_{\xi\xi}[n] - \boldsymbol{R}_\text{mod}\boldsymbol{R}_{\xi\xi}[n] - \boldsymbol{R}_{\xi\xi}[n]\boldsymbol{R}_\text{mod} \\ &+ \boldsymbol{R}_\text{mod}[J_{\min} + \text{tr}(\boldsymbol{R}_{\vartheta\vartheta}[n]\boldsymbol{R}_\text{bloc})] \\ &+ 2\boldsymbol{R}_\text{mod}\boldsymbol{R}_{\xi\xi}[n]\boldsymbol{R}_\text{mod}\end{aligned} \quad (19)$$

where $\boldsymbol{R}_\text{mod}$ is symmetric and positive-definite, hence diagonalizable as $\boldsymbol{R}_\text{mod} = \boldsymbol{Q}\boldsymbol{\Lambda}\boldsymbol{Q}^T$ with $\boldsymbol{Q}^T\boldsymbol{Q} = \boldsymbol{I}_{N_\psi}$ and

$$\boldsymbol{\Lambda} = \text{diag}(\lambda_1, \lambda_2, \ldots, \lambda_{N_\psi}). \quad (20)$$

Pre-multiplying (19) by $\boldsymbol{Q}^T$ and post-multiplying by $\boldsymbol{Q}$ results in

$$\begin{aligned}\boldsymbol{\mathfrak{R}}_{\xi\xi}[n+1] =& \boldsymbol{\mathfrak{R}}_{\xi\xi}[n] - \boldsymbol{\Lambda}\boldsymbol{\mathfrak{R}}_{\xi\xi}[n] - \boldsymbol{\mathfrak{R}}_{\xi\xi}[n]\boldsymbol{\Lambda} \\ &+ \boldsymbol{\Lambda}(J_{\min} + \text{tr}(\boldsymbol{\mathfrak{R}}_{\xi\xi}[n]\boldsymbol{\Lambda})) + 2\boldsymbol{\Lambda}\boldsymbol{\mathfrak{R}}_{\xi\xi}[n]\boldsymbol{\Lambda}\end{aligned} \quad (21)$$

where $\mathfrak{R}_{\xi\xi}[n] = \boldsymbol{Q}^T \boldsymbol{R}_{\xi\xi}[n]\boldsymbol{Q}$.

$\mathfrak{R}_{\xi\xi}[n]$ is an autocorrelation matrix. Then $[\mathfrak{R}_{\xi\xi}[n]]_{i,j}^2 \leq [\mathfrak{R}_{\xi\xi}[n]]_{i,i}[\mathfrak{R}_{\xi\xi}[n]]_{j,j}$, $[\mathfrak{R}_{\xi\xi}[n]]_{i,i} \geq 0$ [25, p. 251], [28], and convergence of (21) can be studied observing only the diagonal elements of $\mathfrak{R}_{\xi\xi}[n]$. Let $[\boldsymbol{\nu}[n]]_i = [\mathfrak{R}_{\xi\xi}[n]]_{i,i}$, $i = 1, \ldots, N_\psi$, denote the vector of diagonal entries of $\mathfrak{R}_{\xi\xi}[n]$ and $\boldsymbol{\lambda} = [\lambda_1, \lambda_2, \ldots, \lambda_{N_\psi}]^T$ be the vector of the eigenvalues of $\boldsymbol{R}_{\text{mod}}$. Then, from (21)

$$[\boldsymbol{\nu}[n+1]]_i = [\boldsymbol{\nu}[n]]_i - 2\lambda_i[\boldsymbol{\nu}[n]]_i + 2\lambda_i^2[\boldsymbol{\nu}[n]]_i + \lambda_i \boldsymbol{\lambda}^T \boldsymbol{\nu}[n] + \lambda_i J_{\min} \tag{22}$$

and

$$\boldsymbol{\nu}[n+1] = \boldsymbol{\Phi}\boldsymbol{\nu}[n] + J_{\min}\boldsymbol{\lambda} \tag{23}$$

where $\text{tr}(\boldsymbol{\Lambda}\mathfrak{R}_{\xi\xi}[n]) = \boldsymbol{\lambda}^T\boldsymbol{\nu}[n]$, $\boldsymbol{\Phi} = \text{diag}(\rho_1, \rho_2, \ldots, \rho_{N_\psi}) + \boldsymbol{\lambda}\boldsymbol{\lambda}^T$ and $\rho_k = (1-\lambda_k)^2 + \lambda_k^2$. The solution to (23) is [29]

$$\boldsymbol{\nu}[n] = \boldsymbol{\Phi}^n\boldsymbol{\nu}[0] + J_{\min}\sum_{j=0}^{n-1}\boldsymbol{\Phi}^j\boldsymbol{\lambda}. \tag{24}$$

Using (24) we now study the stability conditions and the steady-state behavior of (13).

5.1. Stability

Convergence of (24) is determined exclusively by the eigenvalues $\lambda_{\boldsymbol{\Phi}}$ of $\boldsymbol{\Phi}$ [29], which are real and positive. From Gershgorin's theorem [30], a sufficient condition for all $\lambda_{\boldsymbol{\Phi}} < 1$ is

$$\text{tr}(\boldsymbol{R}_{\text{mod}}) = \text{tr}(\boldsymbol{\mathcal{M}}\boldsymbol{R}_{\text{bloc}}) < \frac{2}{3} \tag{25}$$

5.2. Steady State Behavior

When (25) holds, (23) will converge such that $\lim_{n\to\infty}\boldsymbol{\nu}[n+1] = \lim_{n\to\infty}\boldsymbol{\nu}[n] = \boldsymbol{\nu}[\infty]$. Doing as in [4, pp. 326–327] yields

$$J[\infty] = J_{\min}\left[1 + \frac{\frac{1}{2}\sum_{i=1}^{N_\psi}\frac{\lambda_i}{1-\lambda_i}}{1 - \frac{1}{2}\sum_{i=1}^{N_\psi}\frac{\lambda_i}{1-\lambda_i}}\right] \tag{26}$$

where λ_i is the ith eigenvalue in $\boldsymbol{\lambda}$. For $\max\{\lambda_i\} \ll 1$ and $1-\lambda_i \approx 1$ for all i and (26) reduces to

$$J[\infty] \approx J_{\min}\left[1 + \frac{\frac{1}{2}\text{tr}(\boldsymbol{\mathcal{M}}\boldsymbol{R}_{\text{bloc}})}{1 - \frac{1}{2}\text{tr}(\boldsymbol{\mathcal{M}}\boldsymbol{R}_{\text{bloc}})}\right]. \tag{27}$$

Further, if $\text{tr}(\boldsymbol{\mathcal{M}}\boldsymbol{R}_{\text{bloc}}) \ll 2$, (27) yields the simpler approximation $J[\infty] \approx J_{\min}\left[1 + \frac{1}{2}\text{tr}(\boldsymbol{\mathcal{M}}\boldsymbol{R}_{\text{bloc}})\right]$.

6. DIFFERENT BF AND AEC STEP SIZES

So far $\boldsymbol{\mathcal{M}}$ has been required to be positive definite. One interesting choice of $\boldsymbol{\mathcal{M}}$ and $\boldsymbol{B}_{\text{e}}$ is one that permits adaptations of the BF and the AEC using different step sizes. One may choose

$$\boldsymbol{B}_{\text{e}} = \begin{bmatrix} -\boldsymbol{I}_{N_{\text{AEC}}} & \boldsymbol{0}_{N_{\text{AEC}}\times(MN_{\text{BF}}-N_f)} \\ \boldsymbol{0}_{MN_{\text{BF}}\times N_{\text{AEC}}} & \boldsymbol{B} \end{bmatrix} \tag{28}$$

where $\boldsymbol{B}$ is an $MN_{\text{BF}} \times (MN_{\text{BF}} - N_f)$ matrix such that $\boldsymbol{B}^T\boldsymbol{C} = \boldsymbol{0}_{(MN_{\text{BF}}-N_f)\times N_f}$ and $\text{rank}(\boldsymbol{B}) = MN_{\text{BF}} - N_f$, and

$$\boldsymbol{\mathcal{M}} = \begin{bmatrix} \mu_{AEC}\boldsymbol{I}_{N_{\text{AEC}}} & \boldsymbol{0}_{N_{\text{AEC}}\times(MN_{\text{BF}}-N_f)} \\ \boldsymbol{0}_{(MN_{\text{BF}}-N_f)\times N_{\text{AEC}}} & \mu_{BF}\boldsymbol{I}_{MN_{\text{BF}}-N_f} \end{bmatrix}. \tag{29}$$

Then, (13) becomes

$$\hat{\boldsymbol{h}}[n+1] = \hat{\boldsymbol{h}}[n] + \mu_{AEC}d[n]\boldsymbol{u}_{\hat{\text{h}}}[n] \tag{30a}$$

$$\boldsymbol{\psi}_b[n+1] = \boldsymbol{\psi}_b[n] + \mu_{BF}\boldsymbol{B}^T\boldsymbol{x}[n]d[n] \tag{30b}$$

where $\boldsymbol{\psi}_b[n]$ contains the last $MN_{\text{BF}} - N_f$ elements of $\boldsymbol{\psi}[n]$. This is a low complexity implementation that allows to study the behavior of the system under different control logic states.

Using (28) and (29) in (25) yields

$$\mu_{AEC}\text{tr}(\boldsymbol{R}_{\text{u}_{\hat{\text{h}}}\text{u}_{\hat{\text{h}}}}) + \mu_{BF}\text{tr}(\boldsymbol{B}^T\boldsymbol{R}_{\text{x}_\text{b}\text{x}_\text{b}}\boldsymbol{B}) < \frac{2}{3} \tag{31}$$

where $\boldsymbol{R}_{\text{u}_{\hat{\text{h}}}\text{u}_{\hat{\text{h}}}} = E\{\boldsymbol{u}_{\hat{\text{h}}}[n]\boldsymbol{u}_{\hat{\text{h}}}^T[n]\}$ and $\boldsymbol{R}_{\text{x}_\text{b}\text{x}_\text{b}} = E\{\boldsymbol{x}_\text{b}[n]\boldsymbol{x}_\text{b}^T[n]\}$.

7. SIMULATION RESULTS

For model validation, consider a unit power first order autorregressive AR1(-0.9) far-end signal $u[n] = 0.9u[n-1] + z[n]$, 2 microphones, $\mathbf{h}_0$ and $\mathbf{h}_1$ with 500 taps each, generated according to the model in [1]. The desired DOA was assumed orthogonal to the microphone array. The noises $r_0[n]$ and $r_1[n]$ were zero-mean white Gaussian with variance 10^{-2}. The adaptive BF was designed with $N_{\text{BF}} = 16$, linear phase, and all-pass frequency response with $N_f = 16$. The AEC used $N_{\text{AEC}} = N_{\text{h}} + N_{\text{BF}} - 1$. Fig. 3 shows the predicted and simulated transient MOP. We tested 2 scenarios: $[\mu_{AEC}, \mu_{BF}] = [2.6191 \times 10^{-4}, 0.0262]$ and $[\mu_{AEC}, \mu_{BF}] = [3.9840 \times 10^{-4}, 0.0028]$. Fig. 3 shows excellent agreement between theory and predictions in both cases. Counterintuitively, the results show That a larger convergence speed does not necessarily imply a higher steady-state error.

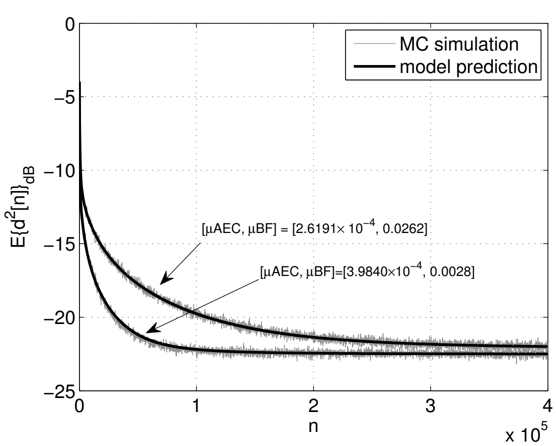

Fig. 3. Monte-Carlo simulation results for 20 runs with AR1(-0.9) input ($M = 2$, $N_{\text{h}} = 500$, $N_{\text{BF}} = 16$ $N_{\text{AEC}} = N_{\text{h}} + N_{\text{BF}} - 1$).

8. CONCLUSIONS

This paper has studied the performance of the adaptive GSC beamforming for the general case of a positive definite step size matrix. The new analysis can be used to predict the behavior of the GSC-based BF-AEC system in different control logic states. It permits the study of the interesting case of using a blocking matrix proposed in [10] and a diagonal step-size matrix, for which the BF and AEC can use different step sizes. Simulation results have shown excellent agreement between theory and simulations.

9. REFERENCES

[1] C. Breining, P. Dreiseitel, E. Hänsler, A. Mader, B. Nitsch, H. Puder, T. Schertler, G. Schmidt, and J. Tilp, "Acoustic echo control. An application of very-high-order adaptive filters," *Signal Processing Magazine, IEEE*, vol. 16, no. 4, pp. 42–69, Jul. 1999.

[2] E. Hänsler and G. Schmidt, *Acoustic Echo and Noise Control: A Practical Approach*, Wiley-Interscience, 2004.

[3] D. G. Manolakis, V. K. Ingle, and S. M. Kogon, *Statistical and adaptive signal processing: spectral estimation, signal modeling, adaptive filtering, and array processing*, McGraw-Hill, New York, NY, USA, 2000.

[4] S. Haykin, *Adaptive Filter Theory (2nd Edition)*, Prentice Hall, Sep. 1993.

[5] B.D. Van Veen and K.M. Buckley, "Beamforming: a versatile approach to spatial filtering," *ASSP Magazine, IEEE*, vol. 5, no. 2, pp. 4 –24, Apr. 1988.

[6] H. L. Van Trees, *Optimum Array Processing (Detection, Estimation, and Modulation Theory, Part IV)*, Wiley-Interscience, 1 edition, Mar. 2002.

[7] W. Kellermann, "Strategies for combining acoustic echo cancellation and adaptive beamforming microphone arrays," in *Acoustics, Speech, and Signal Processing, 1997. ICASSP-97., 1997 IEEE International Conference on*, Apr. 1997, vol. 1, pp. 219–222.

[8] W. Herbordt and W. Kellermann, "GSAEC - acoustic echo cancellation embedded into the generalized sidelobe canceller," in *Proc. European Signal Processing Conference (EUSIPCO)*, Sep. 2000, vol. 3, pp. 1843–1846.

[9] W. Herbordt and W. Kellermann, "Limits for generalized sidelobe cancellers with embedded acoustic echo cancellation," in *Acoustics, Speech, and Signal Processing, 2001. Proceedings. (ICASSP '01). 2001 IEEE International Conference on*, 2001, vol. 5, pp. 3241–3244.

[10] W. Herbordt, W. Kellermann, and S. Nakamura, "Joint optimization of LCMV beamforming and acoustic echo cancellation," in *Proc. European Signal Processing Conference (EUSIPCO)*, 2004, pp. 2003–2006.

[11] K.-D. Kammeyer, M. Kallinger, and A. Mertins, "New aspects of combining echo cancellers with beamformers," in *Proc. IEEE Int. Conf. Acoust., Speech, and Signal Processing*, Philadelphia, PA, USA, Mar. 2005, vol. 3, pp. 137–140.

[12] W. Herbordt, S. Nakamura, and W. Kellermann, "Joint optimization of LCMV beamforming and acoustic echo cancellation for automatic speech recognition," in *Acoustics, Speech, and Signal Processing, 2005. Proceedings. (ICASSP '05). IEEE International Conference on*, Mar. 2005, vol. 3, pp. iii/77 – iii/80 Vol. 3.

[13] M. H. Maruo, J. C. M. Bermudez, and L. S. Resende, "Statistical analysis of the jointly-optimized acoustic echo cancellation BF-AEC structure," in *Acoustics, Speech, and Signal Processing, 2013. ICASSP 2013. Proceedings. 2013 IEEE International Conference on*, 2013, pp. 5840–5844.

[14] M. H. Maruo, J. C. M. Bermudez, and L. S. Resende, "Statistical analysis of a jointly optimized beamformer-assisted acoustic echo canceler," *Signal Processing, IEEE Transactions on*, vol. 62, no. 1, pp. 252–265, Jan 2014.

[15] M. Guo, T. B. Elmedyb, S. H. Jensen, and J. Jensen, "Analysis of acoustic feedback/echo cancellation in multiple-microphone and single-loudspeaker systems using a power transfer function method," *Signal Processing, IEEE Transactions on*, vol. 59, no. 12, pp. 5774 –5788, Dec. 2011.

[16] M. Guo, S.H. Jensen, J. Jensen, and S.L Grant, "Analysis of closed-loop acoustic feedback cancellation systems," in *Acoustics, Speech, and Signal Processing, 2013. ICASSP 2013. Proceedings. 2013 IEEE International Conference on*, 2013, pp. 590–594.

[17] M. Kallinger, J. Bitzer, and K.-D. Kammeyer, "Study on combining multi-channel echo cancellers with beamformers," in *Acoustics, Speech, and Signal Processing, 2000. ICASSP '00. Proceedings. 2000 IEEE International Conference on*, 2000, vol. 2, pp. 797–800.

[18] O.L. Frost, III, "An algorithm for linearly constrained adaptive array processing," *Proceedings of the IEEE*, vol. 60, no. 8, pp. 926 – 935, Aug. 1972.

[19] L. Godara and A. Cantoni, "Analysis of constrained LMS algorithm with application to adaptive beamforming using perturbation sequences," *Antennas and Propagation, IEEE Transactions on*, vol. 34, no. 3, pp. 368 – 379, Mar. 1986.

[20] W. B. Mikhael, F. H. Wu, L. G. Kazovsky, G. Kang, and L. Fransen, "Adaptive filters with individual adaptation of parameters," *Circuits and Systems*, vol. 33, pp. 677–686, 1986.

[21] M. Rupp and J. Cezanne, "Robustness conditions of the LMS algorithm with time-variant matrix step-size," *Signal Process.*, vol. 80, no. 9, pp. 1787–1794, Sep. 2000.

[22] R. Dallinger and M. Rupp, "A strict stability limit for adaptive gradient type algorithms," in *Signals, Systems and Computers, 2009 Conference Record of the Forty-Third Asilomar Conference on*, 2009, pp. 1370–1374.

[23] K. Buckley, "Spatial/spectral filtering with linearly constrained minimum variance beamformers," *Acoustics, Speech and Signal Processing, IEEE Transactions on*, vol. 35, no. 3, pp. 249 – 266, Mar. 1987.

[24] L. Griffiths and C. Jim, "An alternative approach to linearly constrained adaptive beamforming," *Antennas and Propagation, IEEE Transactions on*, vol. 30, no. 1, pp. 27 – 34, Jan. 1982.

[25] A. Papoulis and S. U. Pillai, *Probability, Random Variables, and Stochastic Processes*, McGraw-Hill series in electrical and computer engineering. McGraw-Hill Education, 2002.

[26] D. S. Bernstein, *Matrix Mathematics. Theory, Facts, and Formulas with Application to Linear Systems Theory.*, Princeton University Press, 2005.

[27] R. A. Horn and C. R. Johnson, *Matrix Analysis*, Cambridge University Press, 1990.

[28] J. E. Prussing, "The principal minor test for semidefinite matrices," *AIAA Journal of Guidance, Control, and Dynamics*, vol. 9, no. 1, Jan. 1986.

[29] T. Kailath, *Linear Systems*, Prentice-Hall, New Jersey, USA, 1980.

[30] R. A. Brualdi and S. Mellendorf, "Regions in the complex plane containing the eigenvalues of a matrix," *American Mathematical Monthly*, vol. 101, no. 10, pp. 975–985, Dec. 1994.